# Fourier Spectral of PalmCode as Descriptor for Palmprint Recognition

Meiru Mu[1,2], Qiuqi Ruan[1], Luuk Spreeuwers[2] and Raymond Veldhuis[2]
[1]*Institute of Information Science, Beijing Jiaotong University, Beijing, China*
[2]*Signals and Systems group, University of Twente, Enschede, The Netherlands*

Keywords: Gabor Filtering, Palm Code, Fourier Spectral, Horizontal and Vertical 2DPCA, Palmprint Recognition.

Abstract: Study on automatic person recognition by palmprint is currently a hot topic. In this paper, we propose a novel palmprint recognition method by transforming the typical palmprint phase code feature into its Fourier frequency domain. The resulting real-valued Fourier spectral features are further processed by horizontal and vertical 2DPCA method, which proves highly efficient in terms of computational complexity, storage requirement and recognition accuracy. This paper also gives a contrast study on palm code and competitive code under the proposed feature extraction framework. Besides, experimental results on the Hongkong PolyU Palmprint database demonstrate that the proposed method outperforms many currently reported local Gabor pattern approaches for palmprint recognition.

## 1 INTRODUCTION

Nowadays, recognition of individuals by means of biometric characteristics is becoming increasingly familiar and accepted. The selection of biometrics is commonly application-dependent (D. Zhang, 2004; S. Pankanti et al., 2000). Palmprint, extracted from person's hand, has been recognized as a means of measurement that can uniquely represent a person (W. Shu et al., 1998b). It has been a long history since the palmprints found on the crime scene were used for forensic investigation. Recently, palmprint is being investigated intensively for personal recognition in different real-time application system, such as access control, network security, and social security. Compared with the fingerprints, palmprints have more rich features which are less likely to be destroyed and forged. Besides, palmprints can be captured with a much lower resolution imaging sensor (less than 100 dpi), which leads to be more efficient (W. Shu et al., 1998a). The online palmprint capture devices are mainly based on CCD camera or digital scanner. More recently, the real time multispectral palmprint capture device has also been developed (R.K. Rowe et al., 2007; Z. Guo et al., 2010). In addition to the efficient palmprint acquisition, robust palmprint representation is another key issue for the success of palmprint recognition application.

The algorithms proposed for online palmprint recognition (including verification and identification), are generally divided into three main classes: subspace learning methods, texture energy feature extraction, and coding based methods. Among them, coding based methods are deemed to be the most promising due to their high recognition accuracy and small feature size, which typically involve steps of filter bank selection, coding scheme design and template matching approach. The popular filters include Gabor, Gaussian, and other self-designed ones. The phase, orientation, and magnitude information are generally regarded as encoded objects. The coding rules are usually flexible and simple, and the obtained code features should be robust and provide high discriminative ability. PalmCode (D. Zhang et al., 2003) encodes the phase of Gabor filtered responses into binary features. FusionCode (A. Kong et al., 2006) used a fusion rule at feature layer to further improve PalmCode. DoG code method (X.Q. Wu et al., 2006) first convolves the image using two-dimensional Gaussian filter and then encodes the zero-crossing information of horizontal and vertical gradient values, respectively. OrdinalCode (Z.N. Sun et al., 2005) encodes the outputs of the elliptical Gaussian filters. The schemes encoding the orientation of palm lines are also popular due to its stability which includes competitive code (CompCode) (A. Kong et al., 2004), binary orientation co-occurrence vector (BOCV) code (Z. Guo et al., 2009), palmprint orientation code (POC) (X.Q. Wu et al., 2005), robust line orientation code (RLOC) (W. Jia et al., 2008), and so on (F. Yue et al., 2009; W. Zuo



Mu M., Ruan Q., Spreeuwers L. and Veldhuis R. (2013).
Fourier Spectral of PalmCode as Descriptor for Palmprint Recognition.
In *Proceedings of the 2nd International Conference on Pattern Recognition Applications and Methods*, pages 22-32
DOI: 10.5220/0004228000220032
Copyright © SciTePress

et al., 2010). However, coding based methods require the pixel-to-pixel paired matching between enrollment and query templates. In order to offset the inter-class translation variation, one template has to be shifted in some range and the matching score computation is proceeded multiple times to finally determine the identity of one query palmprint, which is time costly. Refer to Ref. (D. Zhang, 2004), the matching speed of PalmCode is 1.7 ms when the system works under the verification mode and the algorithm is implemented in Visual C++ 6.0 on a PC using Intel Pentium III processor (500MHZ). For identification, if the database contains 100 persons and three palmprint images are registered for each subject, the total identification time is about 1.1s. As can be seen, the matching speed of coding based methods is not desirable for the identification system with large registered database. This issue has also been addressed in some other reported literatures. In order to deal with it, Jia (W. Jia et al., 2008) applied Tensor LPP on their extracted directional representation. However, it can not provide translation invariant performance by reducing the dimension of integer codes directly. Yue (F. Yue et al., 2011) proposed an approach to speed up the coding based palmprint recognition method by building a template tree to perform fast nearest neighbor searching. For both of these methods, the final classification is still based on pixel-to-pixel code template matching by Hamming distance.

Accordingly, in this paper, we aim to further study the code features for palmprint representation. The following three issues are mainly considered:

Firstly, about the filter selection, Gabor, Gaussian, and the second derivative of Gaussian filter have been evaluated based on several coding based methods in Ref. (F. Yue et al., 2008) and their experimental results show that the Gabor filter is superior. Besides, it is well known that Gabor representation can provide optimal localization of image details in a joint spatial and frequency domain (J. Beck, 1987). Concerning these conclusions, the Gabor filters are chosen for our proposed feature extraction method in this paper.

Secondly, about the encoded object, we employ the phase information. Gabor phase, as a discriminating information source, has been successfully used in pattern recognition field. Besides PalmCode and IrisCode, kinds of local Gabor phase pattern operators (W. Zhang et al., 2009; B. Zhang et al., 2007; S. Xie et al., 2010) are proposed as well based on the combination of the spatial histogram and the Gabor phase pattern encoding scheme. These methods involve a group of Gabor filters (in general 40 Gabor filters) to extract the multi-scale and multi-orientation information, which is an overcomplete representation with a high redundant ratio. The high dimensionality of the local Gabor phase pattern histograms leads to high computational cost and large storage requirement. To deal with this problem, this paper proposes a new method, which uses only two Gabor filters while provides higher recognition performance.

Thirdly, instead of representing palmprint image by the code features directly, we transform the code feature matrices into their Fourier frequency fields since a shift in the time domain causes no change in the Fourier magnitude spectrum. The resulting spectral features not only keep the property of powerful discriminative ability of PalmCode features, but also make it possible to extend the application field of coding based features. Because the dissimilarity measurement of the original coding based features is generally based on pixel-to-pixel matching by using Hamming or angular distances, which limits their application to unsupervised template matching mode, while the real-valued spectral features might be processed further by the currently reported supervised learning algorithms, which probably achieves higher recognition performance.


Figure 1: Flow chart of the proposed method. (DFT - discrete Fourier transform; 2DPCA - two-dimensional principle components analysis).

Taking all the above factors into consideration, a novel Fourier spectral representation of PalmCode (DFT_PalmCode) is proposed for palmprint recognition in this paper, whose flow chart is shown in Fig. 1. We firstly transform the typical palmprint phase code feature into its Fourier frequency domain by discrete Fourier transform (DFT). The resulting real-valued Fourier spectral features are then processed by the horizontal and vertical two-dimensional principal component analysis ($(2D)^2$PCA) method. The translation invariant property of Fourier transform and $(2D)^2$PCA dimensionality reduction method help alleviating the within-class image translations to some extent. Compared with the original PalmCode method, the proposed feature extraction approach operates two pairs of Gabor filtering phase responses, which improves the recognition performance evidently. This paper also gives a contrast study on CompCode under the proposed feature extraction framework. For CompCode, palm line orientation information is encoded into bits. Furthermore, our experimental results demonstrate that the proposed method outperforms many currently reported local Gabor pattern operators for palmprint recognition by higher accuracy, lower computational cost and

less storage requirement.

This paper is organized as follows. In section 2, we give a short review of PalmCode. Section 3 illustrates the proposed Fourier spectral representation in details. In section 4, the (2D)$^2$PCA method is described for the dimensional reduction of the proposed spectral features, which helps alleviating the negative effects due to image translation. The experimental results will be demonstrated in section 5. The final part is about the conclusions.

## 2 REVIEW OF PalmCode

The Gabor phase quadrant demodulation coding method is proposed by Daugman for iris recognition in 1993 (J. Daugman, 1993), which is then reported successful for palmprint representation in Ref. (W.K. Kong et al., 2003). For ease of presentation, this feature extraction method is commonly named by IrisCode, PalmCode or Daugman's method.

For PalmCode, a circular 2-D Gabor filter is used to firstly convolve the original gray palmprint image, which has the following general form:

$$g(x,y,u,\theta,\sigma) = \frac{1}{2\pi\sigma^2}\exp\left\{\frac{-(x^2+y^2)}{2\sigma^2}\right\} \times \exp\{2\pi i(ux\cos\theta + uy\sin\theta)\}. \quad (1)$$

Where $i=\sqrt{-1}$, $u$ is the frequency of the sinusoidal wave along the direction $\theta$ from the x-axis, and $\sigma$ specifies the Gaussian envelope along $x$ and $y$ axes, which determines the bandwidth of the Gabor filter. In practice, a Gabor function with a special set of parameters $\{u,\theta,\sigma\}$, is transformed into a discrete Gabor filter. In order to provide more robustness to brightness, the Gabor filter is turned to zero direct current (DC) denoted by $\tilde{g}(x,y)$. Following the experimental setting in Ref. (W.K. Kong et al., 2003), $\sigma$ is set to 5.6179.

Given an image $f(x,y)$ of size $M\times N$, its Gabor filtered images are defined as:

$$G(x,y) = \sum_{x_1}\sum_{y_1} f(x_1,y_1)\cdot\tilde{g}(x-x_1,y-y_1). \quad (2)$$

Where $G(x,y)$ is complex number with real part $\mathtt{Re}(G(x,y))$ and imaginary part $\mathtt{Im}(G(x,y))$.

Assuming the Gabor parameters $\{\theta,u,\sigma\}$ are given, PalmCode method encodes each pixel in the Gabor filtered image into two bits by the following rules:

$$P^{\mathtt{Re}}(x,y) = \begin{cases} 0, & \text{if } \mathtt{Re}(G(x,y)) < 0; \\ 1, & \text{otherwise}. \end{cases} \quad (3)$$

$$P^{\mathtt{Im}}(x,y) = \begin{cases} 0, & \text{if } \mathtt{Im}(G(x,y)) < 0; \\ 1, & \text{otherwise}. \end{cases} \quad (4)$$

Where $P^{\mathtt{Re}}(x,y)$ and $P^{\mathtt{Im}}(x,y)$ are respectively the encoded real and imaginary binary feature templates.

## 3 FOURIER SPECTRAL OF PalmCode

The discrete Fourier transform (DFT) of a function (image) $p(x,y)$ of size $M\times N$ can be given by $P(u,v)=|P(u,v)|e^{\phi(u,v)}$, where $|P(u,v)|=[R^2(u,v)+I^2(u,v)]^{1/2}$ is called the magnitude spectrum of the Fourier transform, and $\phi(u,v)=\tan^{-1}\left[\frac{I(u,v)}{R(u,v)}\right]$ is called the phase angle or phase spectrum of the transform. $R(u,v)$ and $I(u,v)$ are the real and imaginary parts of $F(u,v)$, respectively.

The Fourier transform has the following translation properties:
If $p(x,y)\Leftrightarrow P(u,v)$,
then

$$p(x-x_0,y_0)\Leftrightarrow P(u,v)e^{-j2\pi(ux_0/M+vy_0/N)} \quad (5)$$

and

$$p(x,y)(-1)^{x+y}\Leftrightarrow P(u-M/2,v-N/2). \quad (6)$$

Equation (5) tells us that a shift in the time domain causes no changes in the magnitude spectrum but only the changes in the phase spectrum of Fourier transform. This property has been widely used to extract translation invariant features in pattern recognition. Equation (6) describes that multiplying $p(x,y)$ by $(-1)^{x+y}$ shifts the original of $P(u,v)$ to frequency coordinates $(M/2,N/2)$, which is the center of the $M\times N$ area occupied by the 2-D DFT. This result is based on the variables $u$ and $v$ having values in the range $[0,M-1]$ and $[0,N-1]$, respectively. In a computer implementation these variables will run from $u=1$ to $M$ and $v=1$ to $N$, in which case the actual center of the transform will be at $u=M/2+1$ and $v=N/2+1$. This property is usually used when visualizing the 2-D Fourier spectrum.

The DFT has the following conjugate symmetry property:

$$P(u,v) = P^*(-u,-v), \quad (7)$$

from which it follows that the spectrum is symmetric about the original:

$$|P(u,v)| = |P(-u,-v)|. \quad (8)$$

Based on the symmetry property, we can only keep half of the Fourier coefficients for image representation.

Figure 2 gives an illustration of the proposed Fourier spectral representation scheme. Figure 2(a)

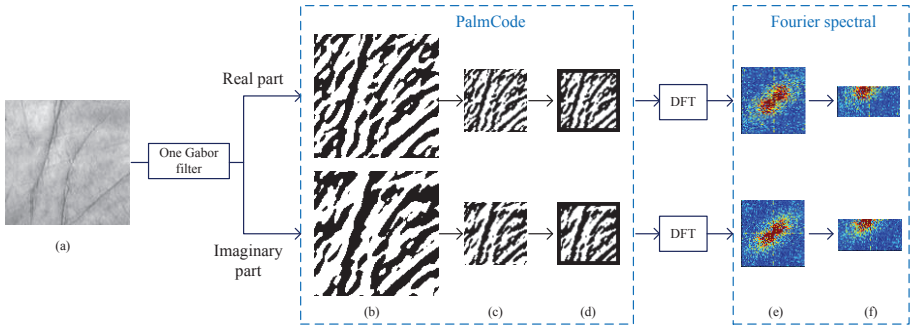


Figure 2: An illustration of the proposed Fourier spectral representation scheme. (a) original image; (b) PalmCode; (c) PalmCode down-sampled by ratio of 2:1; (d) Palmcode with the four rows and columns along the code plane edges set to 0; (e) Fourier spectral of (d); (f) half of (e).

shows a typical palmprint image from PolyU palmprint database. Figure 2(b) visualizes the original PalmCode feature planes as illustrated in section 2. For reducing the computational cost, the PalmCode features are down-sampled by the ratio of 2:1 in this study, as can be seen from Fig. 2(c). On the edge of the code matrices, there are usually some non-palmprint features resulted from defective image preprocessing. For reducing their affects, some masks are generally needed in the classical coding based methods (D. Zhang et al., 2003; A. Kong et al., 2004). While in the proposed method, the values of four rows and columns along the code plane edges are changed into zeros for removing the non-palmprint pixels, as Fig. 2(d) shows. Figure 2(e) shows the Fourier spectral features of PalmCode with the center coordinate $(33,33)$. It is quite obvious that the Fourier spectral matrix is symmetric with respect to the center point. Thus, only half of the spectral values are required for further processing. Figure 2(f) shows half of the spectral features, which is the final Fourier spectral representation of our proposed.

## 4 SPECTRAL FEATURE REDUCTION BY (2D)$^2$PCA

The Fourier spectral feature of PalmCode consists of several real-valued matrices size of $31\times64$, as shown in Fig. 2(f). The large dimensionality leads to high computational cost, limited matching speed and costly template storage requirement. In order to cope with these problems, we resort to (2D)$^2$PCA dimensional reduction technique (X. Pan et al., 2008), which is called Modified 2DPCA (D. Zhang et al., 2009) or horizontal and vertical 2DPCA method (J. Yang et al., 2007) in some other papers. The (2D)$^2$PCA method not only helps saving the computational cost and providing smaller feature space, but also has a useful invariance property: the transform matrix of horizontal 2DPCA is invariant to any change of image row sequence, and the transform matrix of vertical 2DPCA is invariant to any change of an image column sequence. This invariance property of (2D)$^2$PCA helps alleviating the negative effect resulting from image translation (J. Yang et al., 2007). Taking these factors into consideration, (2D)$^2$PCA method is sequently carried out on the Fourier spectral feature space.

Given $N$ spectral feature $X_1, X_2, \ldots, X_N$, each spectral $X_i (i = 1,2,\ldots,N)$ is a $m \times n$ matrix, the goal of horizontal 2DPCA is to find the optimal orthogonal projection axes $U$ so that the projected matrices $Y = [Y_1, Y_2, \ldots, Y_N]$ achieve a maximum total scatter, which can be expressed in the form:

$$Y_i = X_i U, \quad i = 1,2,\ldots,N \tag{9a}$$

$$U = \arg(\max(tr(S_Y))), \tag{9b}$$

where

$$tr(S_Y) = U^T S_X U \tag{10a}$$

$$S_Y = \frac{1}{N}\sum_{j=1}^{N}(Y_j - \bar{Y})(Y_j - \bar{Y})^T \tag{10b}$$

$$S_X = \frac{1}{N}\sum_{j=1}^{N}(X_j - \bar{X})^T(X_j - \bar{X}), \tag{10c}$$

It follows that $S_X$ is a non-negative definite matrix size of $n \times n$. In general, the optimal projection axes $U = [u_1, u_2, \ldots, u_d]$ are chosen as the orthogonal eigenvectors of $S_X$ corresponding to the largest eigenvalues $\lambda_1, \lambda_2, \ldots, \lambda_d$. Thus the projected vectors are $d$-dimensional. Finally, after processed by the horizontal 2DPCA, each spectral matrix is represented as a matrix $Y_i$ of dimension $m \times d$ $(d \ll n)$.

After the procedure of horizontal 2DPCA transform, the correlation between row vectors of spectral feature matrices is removed, and the resulted projection matrices are less sensitive to the translation and

mirror variations of the spectral row sequences. Further, the vertical 2DPCA transform is needed to remove the correlation between column vectors of the projected matrices $Y_i$.

For simplify, the horizontal 2DPCA transform is processed on the transpose of the projected matrices, denoted by $Y_i^T (i = 1,2,\ldots,N)$. Then the corresponding total scatter matrix can be expressed in the form:

$$\begin{aligned} C_{Y^T} &= \frac{1}{N}\sum_{j=1}^{N}(Y_j^T - \bar{Y}^T)^T(Y_j^T - \bar{Y}^T) \\ &= \frac{1}{N}\sum_{j=1}^{N}(Y_j - \bar{Y})(Y_j - \bar{Y})^T, \end{aligned} \tag{11}$$

which is a non-negative definite matrix size of $m \times m$. Let $V = [v_1, v_2, \ldots, v_q]$ be the orthogonal eigenvectors of $C_{Y^T}$ corresponding to the largest eigenvalues $\gamma_1, \gamma_2, \ldots, \gamma_q$ $(q \ll m)$. By letting $R$ represent the projected matrices of $Y$ after the vertical 2DPCA transform, we have $R^T$ is the projected matrices of $Y^T$ after the horizontal 2DPCA transform, that is

$$R^T = Y^T V. \tag{12}$$

It follows that

$$R = (Y^T V)^T = V^T Y = V^T X U, \quad R \in \mathbb{R}^{q \times d}. \tag{13}$$

As can be seen, the dimensionality of the Fourier spectral feature $X$ is reduced from $m \times n$ to $q \times d$ $(d \ll n, q \ll m)$ after the (2D)$^2$PCA transform.

As Fig. 2 shows, each image generates two spectral feature matrices when one Gabor filter is convolved. Based on the proposed feature extraction framework, we might obtain more robust feature representation for palmprint recognition, if more Gabor filters with different orientations are used. As a matter of fact, we find that the proposed method performs much better when two Gabor filters instead of one are used for spectral feature extraction according to the experimental results. Figure 3 illustrates the training steps of the proposed algorithm when two Gabor filters are used, in accordance with which we summarize the proposed palmprint feature extraction algorithm as follows:

Step 1. Input the training palmprint images, and convolve each image with two Gabor filters of different orientation parameters to obtain four PalmCode matrices.

Step 2. Perform the 2-D Fourier transform on each binary PalmCode matrix to get the corresponding spectral feature matrix as described in Fig. 2.

Step 3. Perform (2D)$^2$PCA transform on these spectral feature matrices got in Step 2 to obtain the corresponding four groups of feature projection matrices $(V1,U1)$, $(V2,U2)$, $(V3,U3)$, $(V4,U4)$ as shown in Fig. 3.

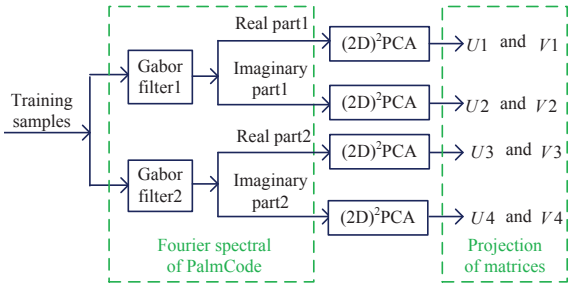


Figure 3: The training steps of the proposed algorithm when two Gabor filters are used. The Fourier spectral of PalmCode is achieved as illustrated in Fig. 2.

Step 4. Transform the four Fourier spectral matrices of each training image by the four groups of feature projection matrices respectively to generate four feature matrices as described in Eq. (13), denoted by $\{$R1,R2,R3,R4$\}$. Save them as the training feature database.

Step 5. When a query image is captured, the same processing as Steps 1 and 2 is applied, and then transform their Fourier spectral matrices as Step 4 to get the final feature template $\{R1', R2', R3', R4'\}$.

Step 6. For template matching, the training and test feature matrices are respectively converted into vectors $\{\overline{R}1, \overline{R}2, \overline{R}3, \overline{R}4\}$ and $\{\overline{R}1', \overline{R}2', \overline{R}3', \overline{R}4'\}$; Then the dissimilarity is measured by sum of Euclidean distance between each pair of vectors $\overline{R}i$ and $\overline{R}i'$, which can be denoted by $\sum_{i=1}^{4} D(\overline{R}i, \overline{R}i')$.

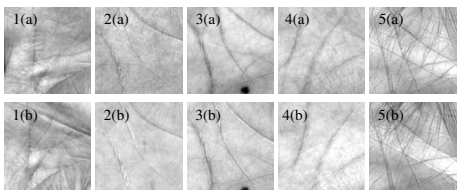


Figure 4: The palmprint images in the Hong Kong PolyU database. (a) Samples in session one; (b) Samples in session two.

## 5 EXPERIMENTAL RESULTS

In this section, we evaluate the recognition performance of our proposed method using HongKong Polytechnic University (PolyU) Palmprint Database, which contains 7752 grayscale images in BMP image

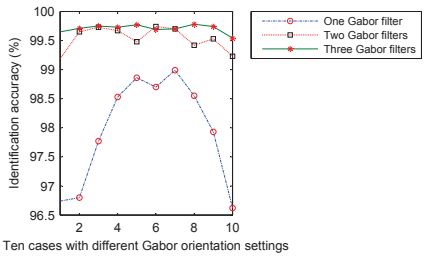


Figure 5: The identification accuracies (%) versus the ten Gabor orientation setting cases.

format. They were captured by CCD camera from 386 different palms and collected in two occasions with different illumination conditions. The interval between the two sessions is about two months. Each person provided around ten palmprint images from the left and right hands respectively. The resolution of original captured images is 384×284 pixels at 75 dpi. By performing the similar preprocessing approach described in Ref. (W.K. Kong et al., 2003), we cropped the region of interest (ROI) size of 128×128. Figure 4 shows the cropped images from five typical palm samples, in which (a) and (b) denote the samples captured from the same palm at the first and second sessions respectively.

## 5.1 Determination of the Parameters

For the Gabor based methods, there is generally a set of adjustable parameters. For DFT_PalmCode method, Besides Gabor parameters, $d$ and $q$ for $(2D)^2$PCA transform are controllable as well. In this group of experiments, we firstly calculate the values $d$ and $q$ by taking 90% of the total sum of the eigenvalues. Based on the obtained values $d$ and $q$, a series of experiments is carried out to investigate the influence of Gabor orientation parameter and examine how the number of Gabor filters affects the identification rate. Secondly, with the determined optimal Gabor filters, the identification accuracies are investigated as $d$ and $q$ vary.

For each palm, five samples from session one are randomly collected to construct the training set, and all the samples (in total 3863) captured in session two are used for testing. Assuming the system is operated in the identification mode (one-to-many comparison). The average correctness rate (%) of ten-run identification executions is used to evaluate the identification performance.

By following the experimental results of literature (W.K. Kong et al., 2003), the Gabor parameter $u$ is set to 0.0916, and $\sigma$ is fixed to 5.6179. In order to determine the optimal number of Gabor filters and their orientation parameters for our proposed method,

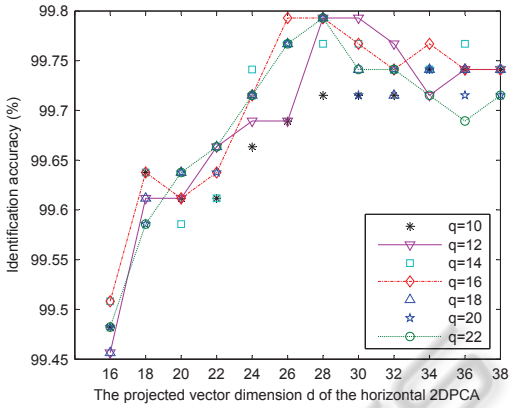


Figure 6: Identification rates (%) as values $d$ and $q$ vary.

we test some orientation cases on palmprint identification accuracy. For the applied $(2D)^2$PCA transform, values $d$ and $q$ are determined by taking 90% of the total sum of eigenvalues. When one Gabor filter is used, the considered orientation values are 0°, 10°, 30°, 45°, 60°, 90°, 120°, 135°, 150°, and 170°, respectively. Besides, the identification rates are also investigated when two and three Gabor filters are used with ten cases of different orientation settings. The tested orientation groups are as follows: {45°, 60°}, {45°, 90°}, {45°, 120°}, {45°, 135°}, {60°, 90°}, {60°, 120°}, {60°, 135°}, {90°, 120°}, {90°, 135°}, {120°, 135°}, {45°,60°, 90°}, {45°, 60°, 120°}, {45°, 60°,135°}, {45°, 90°, 120°}, {45°, 90°, 135°}, {45°, 120°, 135°}, {60°, 90°, 120°}, {60°, 90°, 135°}, {60°, 120°, 135°}, {90°, 120°, 135°}. Figure 5 gives an illustration of the relationship between the identification accuracies and the Gabor orientation parameters. As it shows, the recognition performances of the proposed method improve when the Gabor filter number increases from two to three in most cases. However, the increase of Gabor filter numbers adds to the computational cost in multiple. Based on an overall consideration of the recognition performance and the computational complexity, case 6 with two Gabor filters is determined to be optimum. That is to say, our proposed method achieves the highest identification rate 99.74% when two Gabor filters with the orientation parameters of 60° and 120° respectively are used for the spectral feature extraction on the PolyU palmprint database.

Given the Gabor parameters we got above, the optimal values $d$ and $q$ for $(2D)^2$PCA are experimentally investigated by varying $q$ from 10 to 22 and $d$ from 16 to 38. The identification rates corresponding to different $d$ and $q$ are plotted in Fig. 6. As can be seen, the best identification rate of our proposed method is close to 99.8%. The feature dimension after $(2D)^2$PCA transform is $q \times d$, which is expected to

Table 1: Comparisons of the average identification accuracy (%), time cost (s) for identifying per test sample, and the verification EER (%).

| Method | Identification accuracy (%) | Time cost (s) | Verification EER (%) |
|---|---|---|---|
| PalmCode 0 | 75.63 | 0.067 | 29.5 |
| PalmCode [-1,1] | 95.14 | 0.644 | 9.1 |
| PalmCode [-2,2] | 98.27 | 1.66 | 3.1 |
| DFT_PalmCode | 99.74 | 0.123 | 0.7 |
| CompCode 0 | 78.14 | 0.085 | 24.2 |
| CompCode [-1,1] | 96.17 | 0.920 | 7.2 |
| CompCode [-2,2] | 99.11 | 2.398 | 1.9 |
| DFT_CompCode | 99.29 | 0.106 | 0.9 |

as small as possible while keeping the highest identification rate. Therefore, the best identification performance is obtained when $d = 28$, $q = 12$, as can be seen from Fig. 6.

It should be pointed out that in other experiments we simply take the sum of the largest $d$ eigenvalues that determine 90% of the total sum of the eigenvalues when processing the horizontal 2DPCA transform. By the same way, we get the value of $q$ for the vertical 2DPCA transform.

## 5.2 Comparisons with Coding Methods

In this section the palmprint identification and verification performances are investigated when PalmCode is replaced by the CompCode, which I denote by DFT_CompCode. For PalmCode, the used Gabor filter parameters are given by $u = 0.0916$, $\theta = \pi/4$, and $\sigma = 5.6179$; For CompCode, six Gabor filters are used to obtain the competitive code features with the orientation set as $\theta_j = \pi j/6$, $j = 0, 1, \ldots, 5$. $u$ and $\sigma$ are fixed to 0.0916 and 5.6179 respectively; All the code features mentioned here are down-sampled by ratio of 4:1. For obtaining the matching distance, the code feature matrix needs to be shifted by rows and columns. Here the shifting ranges are set to 0, [-1,1] and [-2,2]. Time cost for identifying per test sample is recorded by Matlab 7.5 from a personal computer with an Intel Pentium(R) Dual-Core Processor (E5200@2.50GHz) and 2GB RAM configured with Microsoft Windows XP.

When the system works in the identification mode, five samples from session one are randomly collected to construct the training set, and all the samples from session two are used for testing. The average identification rates (%) of ten-run executions with different methods are listed in Table 1. Besides, the time cost of identifying one test sample is also compared under the current data set. When the system operates in the verification mode, all the 7752 samples are used. Each palmprint template is matched with all the other ones to evaluate the receiver operating characteristics (ROC). A genuine matching is defined as the matching between the features from the same palm, and otherwise the matching is counted as an impostor. The total number of matches is 30 042 876, of which the number of genuine is 74 068 and the number of impostor is 29 968 808.

Table 1 shows the comparisons of the average identification accuracy (%), time cost (s) for identifying per test sample, and the verification EER (%). As can be seen, the recognition performance of coding based methods depends badly on the translation extent of code feature plane. Furthermore, the matching speed dramatically drops as the translation range increases. The identification rate of CompCode achieves 99.11% at the time cost of 2.398 seconds, which is not desirable when the system is operated in the identification mode. DFT_PalmCode outperforms PalmCode significantly in terms of identification performance and verification accuracy because of two reasons. First, DFT_PalmCode fuses more phase information from two Gabor filters with different orientations, instead of one Gabor filtering as PalmCode exploits, which makes the discriminative ability more powerful. Second, using the frequency-domain representation of code features makes it capable of undergoing training process by some learning algorithms, which improves the recognition performance and also reduces the time cost of dissimilarity calculation. By comparing the identification performances of CompCode and DFT_CompCode, it can be seen that the identification accuracy does not improve evidently while the matching speed drops dramatically after executing DFT transform and $(2D)^2$PCA on the code features. This may be because the processes of DFT transform and $(2D)^2$PCA do not extract more discriminative information from the image, but their resulting real-valued feature templates cost less than the logical-valued code feature planes. From Table 1 it can be also seen that lower EER is achieved by operating the DFT and $(2D)^2$PCA transform on the code features. Since the matching score measurements for coding based methods and the proposed feature repre-

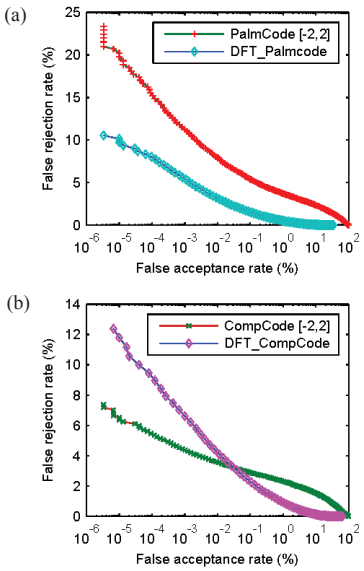


Figure 7: Comparison of the verification accuracies (%) (FAR versus FRR). For the coding based methods, the code template is shifted horizontally and vertically for multiple times within a range [-2, 2].

sentation framework are totally different, we plot their ROC curves for comparisons further. From Fig. 7(a) and (b), we can see that DFT_CompCode does not improve the verification accuracy of CompCode absolutely though it does achieve lower EER. However, DFT_PalmCode does perform much better than PalmCode.

## 5.3 Comparisons with other Methods

Gabor filtering based methods have been widely investigated in various image representation field. Besides coding based methods, there are two other classes: First, Gabor coefficients based statistical learning methods, which make the statistical analysis of the Gabor magnitude coefficients (R. Chu et al., 2007; X. Pan et al., 2008; X. Pan et al., 2009; M. Mu et al., 2011); Second, local Gabor pattern histogram methods (W. Zhang et al., 2009; B. Zhang et al., 2007; S. Xie et al., 2010; W.C. Zhang et al., 2005), which fuse the Gabor coefficients with different local pattern operators to achieve histogram sequences as descriptors. In this section, comparisons with some of them are evaluated on the palmprint recognition performance. Note that for principal component analysis (PCA) and linear discriminant analysis (LDA) involved in these methods, we take the sum of the first largest eigenvalues that determine 90% of the total sum of the eigenvalues for fair comparisons.

GM_(2D)$^2$PCA (X. Pan et al., 2008), as a representative method of Gabor coefficients based statistical learning methods, is compared in this group of experiments. A bank of five-scale and eight-directional filters (in total 40 filters) is firstly used to derive a Gabor feature space of high dimensionality and then two steps of 2DPCA as described in section 4 are carried out to reduce the dimension. The Gabor parameters are set as follows: $\theta_j = \pi j/8$, $j = 0,1,\ldots,7$, $u_v = 0.2592/\sqrt{2^v}$, $v = 0,1,\ldots,4$, $\sigma = 5.6179$. For GM_(2D)$^2$PCA method, the Gabor coefficients are down-sampled by the ratio of 4:1. Otherwise, the Gabor feature dimensionality will be too high to be processed further in our experimental system.

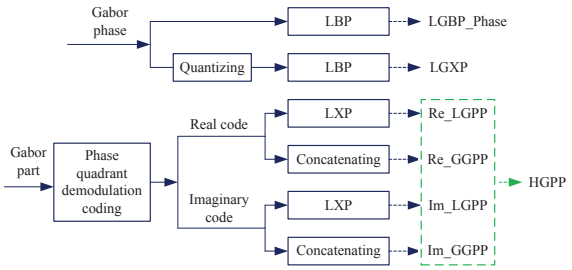


Figure 8: An illustration of various local pattern operators compared in this paper. (LBP - local binary pattern, LXP - local XOR pattern).

By encoding Gabor magnitude and phase coefficients via local binary pattern (LBP) operator, LGBP_Mag (W.C. Zhang et al., 2005) and LGBP_Pha (W. Zhang et al., 2009) have been proposed respectively. By using the local XOR pattern (LXP) operator to encode the real and imaginary parts of Gabor complex response, local Gabor phase pattern (LGPP) has been proposed (B. Zhang et al., 2007), denoted by Re_LGPP and Im_LGPP respectively. Different from LGPP, GGPP has been proposed to represent orientation patterns, which forms one eight-bit binary string to represent each pixel by concatenating the real or imaginary quadrant-bit codes of different orientations for a given frequency (denoted by Re_GGPP and Im_GGPP). In addition, Xie (S. Xie et al., 2010) proposed local Gabor XOR pattern (LGXP) by quantizing the Gabor phase in each local region firstly, and then encoding the quantized phases by LXP operator. Figure 8 gives an illustration of different local Gabor pattern operators. For fair comparisons, the Gabor parameters used in all the mentioned local Gabor pattern methods are the same as those set in GM_(2D)$^2$PCA method.

We assume that the system works in the identification mode, samples from session one are used for training, and all the samples from session two for test. Different training sets are constructed respectively with the sample numbers of each palmprint class ranging from two to five. The training samples are randomly selected and ten-run executions are av-

Table 2: Comparisons of the average identification accuracy (%) and feature length among different methods. For evaluating the identification performance, the training sample number per class ranges from two to five. The average identification rate is calculated over ten-run executions with various training and testing sets.

| Method | Identification rate (%) | | | | Gabor number | Feature length before reduction | Final feature length |
|---|---|---|---|---|---|---|---|
| | 5 | 4 | 3 | 2 | | | |
| DFT_PalmCode | 99.74 | 99.67 | 99.55 | 99.24 | 2 | 7 936 | 2 878 |
| GM_$(2D)^2$PCA | 81.42 | 80.34 | 77.65 | 74.84 | 40 | 40 960 | 13 680 |
| Re_LGPP | 97.10 | 96.87 | 96.20 | 94.18 | 40 | 40 960 | 1 540 |
| Im_LGPP | 97.22 | 97.10 | 96.56 | 95.48 | 40 | 40 960 | 1 540 |
| HGPP | 98.40 | 98.11 | 97.93 | 97.82 | 40 | 92 160 | 1 540 |
| LGBP_Phase | 97.75 | 97.57 | 97.08 | 95.92 | 40 | 40 960 | 1 540 |
| LGXP | 98.24 | 97.97 | 97.42 | 97.15 | 40 | 40 960 | 1 540 |

eraged to evaluate the identification rate (%). Besides, the resulting feature size is also investigated for evaluating the computational complexity.

Table 2 lists the comparisons of palmprint identification performance. As it shows, the proposed method achieves the highest identification rate by a large margin. Even under the condition of less training samples, the identification accuracy of DFT_PalmCode method reaches up to 99.24%. Different from the other Gabor based methods, which extract multi-scale and multi-directional features using 40 Gabor filters, DFT_PalmCode uses only two Gabor filters. Since the Gabor filtering is time-costing, less used filters leads to the advantages of higher execution speed and lower storage requirement. Besides, all the local Gabor pattern methods generate a histogram feature space with high dimensionality. As the number of resulting sub-blocks increases, the histogram dimension will extend in multiple. Given the sub-block number be $N$, and the image class number $C$, then the final feature vector length will be $N \times (C-1)$. As Table 2 shows, $N \times (C-1) = 4 \times (386-1) = 1540$ is the final feature size of the mentioned local Gabor pattern methods in this group of experiments, while the final feature length of DFT_PalmCode is 2878, which is larger but still comparable.

## 6 CONCLUSIONS

In this paper, we have presented a new feature extraction method for palmprint recognition. The Gabor phase information is firstly encoded into binary code features, which are then transformed into Fourier spectral (denoted by DFT_PalmCode) as palmprint descriptor. The spectral features are further processed by the horizontal and vertical 2DPCA transform for palmprint recognition. Experimental results demonstrate its high efficiency under both verification and identification system mode.

The main contributions and conclusions of this paper are as follows: (1) The proposed method is related to the original PalmCode approach, but they are quite different. First, the real-valued spectral features are achieved for palmprint recognition instead of the binary code matrices, which not only keep the high discriminative ability of PalmCode features, but also can be processed by some learning algorithms to further improve the recognition performance. Second, due to the translational invariance property of Fourier and $(2D)^2$PCA transform, DFT_PalmCode method overcomes the weakness of pixel-to-pixel matching strategy, which is widely applied by the coding based methods as well as PalmCode. Third, under the proposed feature extraction framework, more than one Gabor filters can be utilized to fuse phase information, which improves the recognition accuracy evidently compared with PalmCode. (2) The contrast experimental results between another coding method and our method demonstrate that the proposed feature extraction framework can be used on other code-plane based features for increasing identification speed as well as PalmCode. (3) Compared with other state-of-the-art Gabor phase based methods which generally use 40 Gabor filters, the proposed method greatly outperforms in terms of recognition accuracy, computational complexity and storage requirement by using only two Gabor filters.

## ACKNOWLEDGEMENTS

This work is supported partly by the National Grand Fundamental Research 973 Program of China under Grant No. 2004CB318005, and the Fundamental Research Funds for the Central Universities (Grant No. KKJB11034536).

## REFERENCES

Kong, A. and Zhang, D. (Aug. 23-26, 2004). Competitive

coding scheme for palmprint verification. In *Proc. 17th Int. Conf. Pattern Recognition (ICPR'04)*, pages 520–523, Cambridge, UK.

Kong, A. and Zhang, D. and Kamel, M. (2006). Palmprint identication using feature-level fusion,. *Pattern Recognition*, 39(3):478–487.

Zhang, B. and Shan, S. and Chen, X. and Gao, W. (2007). Histogram of gabor phase patterns (hgpp): A novel object representation approach for face recognition. *IEEE Trans. image process.*, 16:57–68.

Han, D. and Guo, Z. and Zhang, D. (Oct.26-29, 2008). Multispectral palmprint recognition using wavelet-based image fusion. In *Proc. Int. Conf. Signal Processing*, pages 2074–2077, Beijing,China.

Zhang, D. and Kong, A. and You, J. and Wong, M. (2003). Online palmprint identification. *IEEE Trans. Pattern. Anal. Mach. Intell.*, 25(9):1041–1050.

Zhang, D. and You, X. and Wang, P. and Yanushkevich, S. N. and Tang, Y. (2009). Facial biometrics using nontensor product wavelet and 2d discriminant techniques. *Int. J. Patt. Recog. Art. Intel.*, 23(3):521–543.

Daugman, J. (1993). High confidence visual recognition of persons by a test of statistical independence. *IEEE Trans. Pattern Anal. Mach. Intell.*, 15(11):1148–1161.

Yue, F. and Zuo, W. and et al.. (2011). Fast palmprint identification with multiple templates per subject. *Pattern Recognition Letters*, 32:1108–1118.

Yue, F. and Zuo, W. and Zhang, D. and Wang, K. (2009). Orientation selection using modified fcm for competitive code-based palmprint recognition. *Pattern Recognition*, 42(11):2841–2849.

Yue, F. and Zuo, W. and Wang, K. and Zhang, D. (Jun. 24-26, 2008). A performance evaluation of filter design and coding schemes for palmprint recognition. In *Proc. 19th Int. Conf. Pattern Recognition (ICPR)*, pages 1–4.

Beck, J. and Sutter, A. and Ivry, R. (1987). Spatial frequency channels and perceptual grouping in texture segmentation. *Computer Vision, Graphics, Image Processing*, 37(1987):299–325.

Yang, J. and Liu, C. (2007). Horizontal and vertical 2dpca-based discriminant analysis for face verification on a large-scale database. *IEEE Transactions on Information Forensics and Security*, 2(4):781–792.

Mu, M. and Ruan, Q. (2011). Mean and standard deviation as features for palmprint recognition based on gabor filters. *Int. J. Patt. Recog. Art. Intel.*, 25(4):491–512.

Chu, R. and Lei, Z. and Han, Y. and He, R. and Li, S. Z. (Nov.18-22, 2007). Learning gabor magnitude features for palmprint recognition. In *Proc. 8th Asian Conf. Computer Vision (ACCV2007)*, pages 22–31, Tokyo, Japan.

Rowe, R. K. and Uludag, U. and Demirkus, M. and Parthasaradhi, S. and Jain, A. K. (Sept.11-13, 2007). A multispectral whole-hand biometric authentication system. In *Proc. Biometrics Symposium*, pages 1–6, Baltimore, MD.

Pankanti, S. and Bolle, R. M. and Jain, A. K. (2000). Biometrics: The future of identification. *IEEE Computer*, 33(2):46–49.

Xie, S. and Shan, S. and Chen, X. and Chen, J. (2010). Fusing local patterns of gabor magnitude and phase for face recognition. *IEEE Trans. Image Process.*, 19(5):1349–1361.

Jia, W. and Huang, D. and Tao, D. and Zhang, D. (12-15 Oct. 2008). Palmprint identification based on directional representation. In *Proc. IEEE Int. Conf. Systems, Man and Cybernetics (SMC2008)*, pages 1562–1567, Singapore.

Jia, W. and Huang, D. S. and Zhang, D. (2008). Palmprint verification based on robust line orientation code. *Pattern Recognition*, 41(5):1521–1530.

Shu, W. and Zhang, D. (1998a). Automated personal identification by palmprint. *Optical Engineering*, 37(8):2659–2362.

Shu, W. and Zhang, D. (Aug.16-20,1998b). Palmprint verification: An implementation of biometric technology. In *Proc. 14th Int. Conf. Pattern Recogn.*, pages 219–221, Brisbane,Australia.

Zhang, W. and Shan, S. and Chen, X. and Gao, W. (2009). Are gabor phases really useless for face recognition? *Pattern Analysis & Applications*, 12(3):301–307.

Zuo, W. and Lin, Z. and Guo, Z. and Zhang, D. (Jun.13-18, 2010). The multiscale competitive code via sparse representation for palmprint verification. In *Proc. 23rd IEEE Int. Conf. Computer Vision and Pattern Recognition (CVPR)*, pages 2265–2272, San Francisco, CA, USA.

Zhang, W. C. and Shan, S. G. and Gao, W. and Zhang, H. M. (Oct.17-21, 2005). Local gabor binary pattern histogram sequence (lgbphs): A novel non-statistical model for face representation and recognition. In *Proc. 10th Int. Conf. Computer Vision*, volume 1, pages 786–791, Beijing, China.

Kong, W. K. and Zhang, D. and Li, W. (2003). Palmprint feature extraction using 2-d gabor filters. *Pattern Recognition*, 36(10):2339–2347.

Pan, X. and Ruan, Q. (2008). Palmprint recognition using gabor feature-based $(2d)^2$pca. *Neurocomputing Letters*, 71(13-15):3032–3036.

Pan, X. and Ruan, Q. (2009). Palmprint recognition using gabor-based local ivariant features. *Neurocomputing Letters*, 72(7-9):2040–2045.

Wu, X. Q. and Wang, K. Q. and Zhang, D. (2005). Palmprint authentication based on orientation code matching. *in: AVBPA 2005, Lecture Notes in Computer Science*, 3546:555–562.

Wu, X. Q. and Wang, K. Q. and Zhang, D. (Nov.3-6, 2006). Palmprint texture analysis using derivative of gaussian filters. In *in: Proc. IEEE Int. Conf. Computational Intelligence and Security*, pages 751–754, Guangzhou, China.

Hao, Y. and Sun, Z. and Tan, T. (Nov.18-22, 2007). Comparative studies on multispectral palm image fusion for biometrics. In *Proc. 8th Asian Conference on Computer Vision (ACCV)*, pages 12–21, Tokyo, Japan.

Guo, Z. and Zhang, L. and Zhang, D. (Aug. 23-26, 2010). Feature band selection for multispectral palmprint recognition. In *Proc. 20th Int. Conf. Pattern Recognition (ICPR)*, pages 1136-1139.

Guo, Z. and Zhang, D. and Zhang, L. and Zuo, W. (2009). Palmprint verification using binary orientation co-occurrence vector. *Pattern Recognition Letters*, 30:1219–1227.

Guo, Z. H. and Lu, G. M. (July 11-14, 2010). Palmprint recognition using gabor magnitude code. In *Proc. IEEE Int. Conf. Machine Learning and Cybernetics (ICMLC)*, volume 2, pages 796–801, Qingdao, China.

Zhang, D. (2004). *Palmprint Authentication*. Kluwer Academic Publication, Dordrecht.

Sun, Z. N. and Tan, T. N. and Wang, Y. H. and Li, S. Z. (Jun.25, 2005). Ordinal palmprint representation for personal identification. In *Proc. IEEE Int. Conf. Computer Vision and Pattern Recognition*, San Diego, CA, USA.

SciTePress
Science and Technology Publications